

Observation of tunneling anisotropy in superconducting niobium crystals

S. M. Durbin, D. S. Buchanan, J. E. Cunningham, and D. M. Ginsberg

Department of Physics and Materials Research Laboratory, University of Illinois at Urbana—Champaign, Urbana, Illinois 61801

(Received 23 May 1983; revised manuscript received 8 August 1983)

Superconducting proximity-effect tunneling measurements have been performed on (110)- and (111)- oriented niobium crystals grown by molecular-beam epitaxy. Measurements of ac resistance yield information about the effective phonon density of states; different results were obtained for the two crystal orientations. *In situ* high-energy electron diffraction studies indicate atomically smooth interfaces in the proximity sandwich and also indicate amorphous-oxide barriers for these junctions. We therefore have a nearly ideal configuration, which may account for the sensitivity to crystal orientation. The failure of the McMillan inversion program to converge for the (111) data suggests the need for a \vec{k} -dependent formulation of the equations.

I. INTRODUCTION

Strong electron-phonon coupling in the transition metal niobium is indicated clearly by anomalous dips in the phonon dispersion curves measured by neutron scattering.¹ Strong anomalies in the [100] and [111] branches of $\omega(q)$ vs q cause two principal peaks in the phonon density of states, $F(\omega)$ vs ω . A direct connection between these phonon features and electronic Fermi-surface structure has been demonstrated theoretically by Varma and Weber.² Superconducting electron-tunneling experiments on Nb have produced effective phonon densities of states, $\alpha^2(\omega)F(\omega)$, where $\alpha^2(\omega)$ is an electron-phonon coupling constant.³ Second-order Raman scattering experiments on molecular-beam-epitaxy— (MBE) grown Nb crystals⁴ have also yielded $F(\omega)$, weighted by a factor of approximately $\alpha^4(\omega)$. Both the tunneling and the Raman results show the two principal phonon peaks at 16 and 23 meV seen in the neutron $F(\omega)$ for the [111] and [100] branches, respectively.

Since these peaks in $F(\omega)$ derive from phonon branches with differing symmetries, superconducting tunneling measurements made on single-crystal Nb samples having different crystal orientations should produce $\alpha^2(\omega, \vec{k})F(\omega, \vec{k})$ depending upon orientation of \vec{k} if the tunneling process is sensitive to crystal anisotropy. Many previous experiments have attempted to show superconducting-gap anisotropies via single-crystal tunneling, but obtained mixed results.⁵ The experiment described here was an attempt to observe anisotropy effects in phonon spectra by fabricating samples with improved interface quality at the tunnel junctions.

II. EXPERIMENTAL METHODS

The Nb crystals used in these tunneling experiments were grown by thermal evaporation from an electron-beam gun in an ultrahigh-vacuum MBE system, described elsewhere.⁶ As previously reported,⁷ Nb grows as a high-quality single crystal with a (110) surface plane on (11 $\bar{2}$ 0)

sapphire substrates, and with a (111) surface on (0001) sapphire. The various samples were deposited at rates of 0.5–5.0 Å/s onto substrates heated to 850°C, with ambient pressures rising to $(1-10)\times 10^{-9}$ Torr during deposition. Nb crystals made this way by us have x-ray-diffraction rocking curves showing widths less than or equal to 0.1°, indicating a good crystal structure. Because proximity-effect tunneling must be used to obtain good tunneling characteristics from Nb, 35 Å of aluminum was deposited onto the fresh Nb surface after the substrate temperature had fallen below 350°C. Bulk interdiffusion should have been negligible; our calculations based on available data⁸ for Al and Nb-Al compounds in Nb show that many days at this temperature would be required for mixing to extend past a single monolayer. Other studies have shown³ that an Al proximity layer of this thickness provides a good, insulating oxide barrier without perceptibly altering the Nb tunneling characteristics.

Tunnel junctions were fabricated by oxidizing the samples in air for 2–3 h at room temperature, masking the edges with an evaporated SiO film and depositing a series of Al counterelectrodes. Junction resistances produced in this manner were typically 100–2000 Ω. Samples were mounted in a cryostat equipped with a ³He refrigerator capable of cooling the samples to T=0.39 K. The tunneling data were obtained at that temperature.

Tunneling characteristics were measured in a conventional fashion with the junction forming one arm of an ac bridge circuit.⁹ A constant dc current biased the junction to a desired voltage, while a small ac current allowed the first- and second-harmonic components of the ac resistance to be detected by lock-in amplifiers, yielding dV/dI and d^2V/dI^2 . The bias voltage and the two lock-in outputs were read by separate digital voltmeters, signal-averaged by an LSI-11 minicomputer, and stored on a magnetic disk.

Resistance measurements were made in 0.15-mV bias intervals from ± 45 to ± 4 mV, with a 0.30-mV peak-to-peak ac voltage component. Conductance (dI/dV) measurements were made in the superconducting-gap regions,

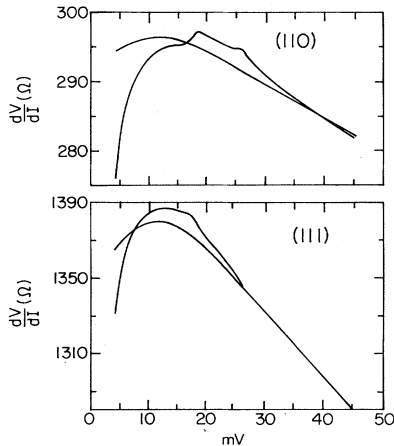


FIG. 1. dV/dI measurements of two Nb samples grown simultaneously on different substrates to produce (110) and (111) crystals. Upper part of figure shows the (110) data; the lower part shows the (111) results. Both the smoother, normal-state dV/dI and the superconducting-state dV/dI are plotted for each sample.

from which values of the energy-gap parameters $\Delta_{\text{Nb}} \approx 1.5$ mV and $\Delta_{\text{Al}} \approx 0.2$ mV were determined. The leakage current at zero bias was typically 1–3% of the current at high bias. Superconducting transition temperatures T_c of the films were determined by monitoring the resistive transition.

III. RESULTS

The difference between our (110) and (111) tunneling results is best illustrated by considering two samples prepared with these orientations under identical conditions by having the two substrates side by side during the deposition process. Table I lists the characteristics of the two samples which we discuss in detail. Figure 1 shows the raw dV/dI data in the superconducting and normal states for both samples. The (110) data are quite similar to results obtained from bulk Nb crystals by Wolf *et al.*,³ while the (111) data are not. The unambiguous difference between the two samples is typical of MBE-produced Nb samples of varying quality; derivative data were obtained from a total of eight junctions on Nb(111) crystals, whose

residual resistivity ratios (room-temperature resistance divided by that just above T_c) ranged from 3 to 186. Behavior which was anomalous, relative to the (110) data, was exhibited by all eight of these junctions, as shown by the (111) data in Fig. 1. Resistivity ratios as high as 186 are quite good for vapor-deposited films, but fall below that of the best bulk crystals. A resistivity ratio of 3 (for which the electron mean free path¹⁰ $l \sim 78$ Å) indicates that the superconducting state can no longer be described in the clean limit, (l much greater than the ideal coherence length). We therefore suggest that the difference between our (110) and our (111) data does not result from an electron mean-free-path effect.

By assuming that the transmission probability T_{12} of a single quasiparticle striking the barrier is independent of energy, the tunneling current can be modeled as¹¹

$$I(V) = |T_{12}|^2 \int_0^\infty N_1(E) N_2(E - eV) \times [f(E) - f(E - eV)] dE,$$

where $N_1(E)$ and $N_2(E)$ are the quasiparticle densities of states on the two sides of the barrier and $f(E)$ is the Fermi-Dirac distribution function. The ratio of the superconducting to the normal density of states is then obtained from the experimental data as

$$\frac{(dI/dV)_S}{(dI/dV)_N} = \frac{N_S(E)}{N_N(E)} \equiv \sigma(E).$$

Stage two of the McMillan inversion program^{12,13} was used to deconvolute the contribution of the Al counterelectrode, yielding $\sigma(E)/\sigma_{\text{BCS}}(E)$ from the raw data, where $\sigma_{\text{BCS}}(E) = E/(E^2 - \Delta^2)^{1/2}$ is the density of quasiparticle states for an ideal weak-coupling superconductor. To further emphasize the deviation from the BCS form, i.e., to accentuate the role of strong electron-phonon coupling, Fig. 2 shows $-d(\sigma/\sigma_{\text{BCS}})/dE$ plotted against bias voltage above the gap energy. The (110) data show peaks at 16 and 23 meV, whereas the (111) results appear to show these two features greatly broadened and slightly softened.

IV. DISCUSSION

Having consistently observed anomalous phonon spectra for Nb(111) tunnel junctions, we now consider various possible causes of the anomalies. A significant unknown factor is the quality of the Nb-Al interface. We had no

TABLE I. Sample characteristics.

Sample	128A	128C
Orientation	(110)	(111)
Deposition rate	2 Å/sec	2 Å/sec
Ambient pressure during deposition	7×10^{-9} Torr	7×10^{-9} Torr
T_c	9.23 K	9.31 K
Residual resistance ratio of film	150	186
Normal-state resistance of junction 3	300 Ω	1390 Ω
Leakage conductance of junction 3 at zero bias and 0.39 K, normalized to high-bias conductance	2.2%	1.0%

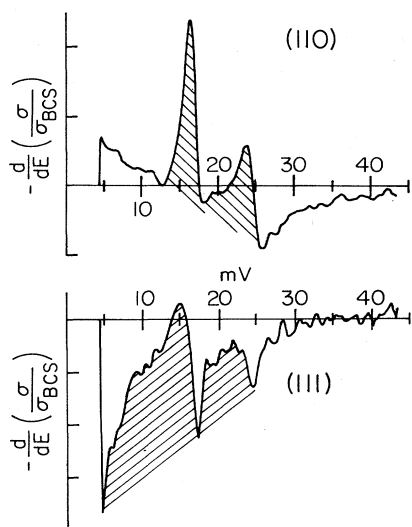


FIG. 2. Plot of $-d(\sigma/\sigma_{\text{BCS}})/dE$ vs bias voltage measured from the gap edge, where σ is the quasiparticle density of states determined from dV/dI measurements. Upper part of figure is derived from the (110) data shown in Fig. 1, and the lower part is from the (111) data. Shaded areas approximately represent the shape of the $\alpha^2 F$ output from these data.

means of determining whether a thin intermetallic compound had formed at the interface, with superconducting properties which perturbed the tunneling. Also, other workers have found that part of an Al overlayer on polycrystalline Nb films can diffuse into the Nb through grain boundaries.¹⁴ We cannot rule out such intermixing, but the high quality of our single-crystal samples should inhibit it. We are confident that Al does completely cover the Nb surface of our samples, because the oxidation time required¹⁵ to form insulating barriers on Nb is much longer than the few hours which was sufficient for our samples.

The nominal 35-Å proximity layer might even have segregated to surface defects while still leaving enough Al to form a continuous oxide. It is not clear how such a composite surface would affect tunneling characteristics. Milkove *et al.*¹⁶ have shown that some "anomalous" tunneling data can be modeled by considering the junction to be two or more different junctions carrying current in parallel, which a composite surface may resemble.

While we cannot exclude such microscopic perturbations, any junction artifact affecting the data must be present only on (111) surfaces. We now consider whether or not the explanation of the (111) data may lie in the intrinsic superconducting properties of Nb.

If a quasiparticle is propagating normal to a perfectly planar barrier, the momentum parallel to the surface is conserved during transmission through the barrier, so that

only final states with $k_{\parallel}=0$ should be occupied. This tunneling selects a subset of the available states $N(E, \vec{k})$. Since the Fermi surface of Nb has three distinct types of highly anisotropic parts,¹⁷ this selection process will depend on orientation. While tunneling is most probable for quasiparticles with $k_{\parallel}=0$, realistic calculations have shown that the angular distribution of tunneling particles typically has a 20° half-width at half maximum, even for ideal barriers.¹⁸ Although this distribution would smear out some crystal-anisotropy effects, it should not be sufficient to confuse the [110] and [111] directions, since they are separated by 35°.

There are several interface-quality problems which, if present, would be sufficient to prevent observation of these effects. Quasiparticle final states would be averaged over \vec{k} near the oxide or proximity interface by incoherent scattering caused by impurities, coherency strains, and other perturbations. Imperfectly planar interfaces would weaken the approximate $k_{\parallel}=0$ selection rule. An orientation dependence of the transmission probability $T_{12}(\vec{k})$ for a crystalline barrier¹⁹ could mask any intrinsic anisotropy due to Nb. To investigate the interface quality of these samples, a high-energy electron-diffraction study was conducted in the MBE growth chamber, which was equipped with a 10-keV electron gun and a phosphor display window for observing glancing-incidence electron-diffraction patterns. Nb and Al were deposited on (0001) and (11 $\bar{2}$ 0) sapphire substrates in the same way the tunnel samples were made, with the following results.

(1) The diffraction spots from Nb(110) and Nb(111) crystals had completely elongated into lines normal to the surface, indicating that these surfaces were single crystalline and "atomically smooth" insofar as electron diffraction indicated.

(2) The Al overlayer formed a (111) epitaxial layer on both orientations of Nb and was also atomically smooth.

(3) After oxidation in air the Al-oxide surface produced an essentially structureless diffraction pattern, suggesting that the insulating barrier was amorphous.

This apparent atomic smoothness indicates the interfaces were indeed planar, so the $k_{\parallel}=0$ selection rule should hold. The amorphous nature of the oxide barrier and the fact that the Al overlayer grows in the same orientation for both orientations of the Nb make the oxide and the overlayer unlikely sources of the observed tunneling anisotropy.

Stage three of the McMillan inversion program uses the experimental $N(E)$ to solve the isotropic Eliashberg equations for $\alpha^2(\omega)F(\omega)$. This program worked well with the (110) data, yielding an $\alpha^2(\omega)F(\omega)$ quite similar to other published results.³ For the (111) data, the program failed to converge. If anisotropic tunneling effects are involved, this failure to converge may arise from the isotropic formulation of the program. A full \vec{k} -dependent treatment would require solutions of²⁰

$$\alpha^2(\omega, \vec{k})F(\omega, \vec{k}) = \frac{1}{(2\pi)^3} \int \frac{dS_{\vec{k}'}}{\hbar v_{\vec{k}'}} \sum_{\lambda} |g_{\vec{k}' \vec{k} \lambda}|^2 \delta(\omega - \omega_{\lambda}(\vec{k}' - \vec{k})),$$

where the integration is over the Fermi surface, $v_{\vec{k}}$ is the Fermi velocity, and $g_{\vec{k}\vec{k}'\lambda}$ is the matrix element for the interaction between electron states \vec{k} and \vec{k}' via a phonon of wave vector $\vec{q} = \vec{k} - \vec{k}'$, energy ω_q , and polarization λ . The anisotropy included in this formulation makes the equations more complicated, and the McMillan inversion program has not been generalized to this case. It should be noted that stage three of the program requires normal-state tunneling data. We obtained these at 10 K, while the superconducting-state data were obtained at 0.39 K. This could also be responsible for the convergence problem.

It is puzzling that the (110) data converge better than the (111) data. If MBE tunneling in anisotropic Nb is \vec{k} dependent, why do the (110) data converge in an isotropic formulation and produce a phonon spectrum essentially the same as that derived from intrinsically isotropic Raman measurements?⁶ It may be that the (110) spectrum fortuitously resembles the isotropic results because the [110] direction is separated by roughly the same angle from the [100] and [111] directions (45° and 35°, respectively).

V. SUMMARY

The data presented here show very different electron-phonon coupling in the tunneling spectra of Nb(110) and

Nb(111) crystals grown by MBE. *In situ* electron-diffraction studies of these tunneling samples have shown atomically smooth proximity interfaces, epitaxial growth of the Al proximity layer, and an apparently amorphous oxide barrier. These nearly ideal barrier properties may permit the tunneling electrons to sense intrinsic crystal-anisotropy effects in Nb, although some possible difficulties cannot be excluded. The failure of the McMillan inversion program to converge for the (111) data may indicate that a \vec{k} -dependent formulation of the Eliashberg equations should be applied to the data.

ACKNOWLEDGMENTS

The preparation and characterization of the samples by two of us (S.M.D. and J.E.C.) were supported by the National Science Foundation under Materials Research Laboratory Grant No. NSF-DMR-80-20250. The acquisition of the tunneling data by the other two of us (D.S.B. and D.M.G.) was supported by the National Science Foundation under Grant No. NSF-DMR-82-03528. One of us (S.M.D.) thanks C. P. Flynn for guidance.

¹Y. Nakagawa and A. D. B. Woods, Phys. Rev. Lett. **11**, 271 (1963).

²C. M. Varma and W. Weber, Phys. Rev. B **19**, 6142 (1979).

³E. L. Wolf, J. Zasadzinski, J. W. Osmun, and G. B. Arnold, J. Low Temp. Phys. **40**, 19 (1980).

⁴M. V. Klein, S. B. Dierker, S. M. Durbin, and C. P. Flynn, in *Superconductivity in d- and f-band Metals*, edited by W. Buckel and W. Weber (Kernforschungszenrum Karlsruhe, Karlsruhe, 1982), p. 569.

⁵J. L. Bostock and M. L. A. MacVicar, in *Anisotropy Effects in Superconductors*, edited by H. W. Weber (Plenum, New York, 1977), p. 213.

⁶S. M. Durbin, Ph.D. thesis, University of Illinois, 1983 (unpublished).

⁷S. M. Durbin, J. E. Cunningham, and C. P. Flynn, J. Phys. F **12**, L75 (1982).

⁸*Diffusion and Defect Data*, edited by F. H. Wohlbley (Trans Tech House, Aebemansdorf, Switzerland, 1976), Vol. 12, pp. 19 and 84.

⁹B. W. Nedrud, Ph.D. thesis, University of Illinois, 1981 (unpublished).

¹⁰A. F. Mayadas, R. B. Laibowitz, and J. J. Cuomo, J. Appl.

Phys. **43**, 1287 (1972).

¹¹J. Bardeen, Phys. Rev. Lett. **6**, 57 (1961).

¹²W. L. McMillan and J. M. Rowell, Phys. Rev. Lett. **14**, 108 (1965).

¹³B. W. Nedrud, University of Illinois Technical Report No. 217 (unpublished).

¹⁴J. Kwo, G. K. Wertheim, M. Gurvitch, and D. N. E. Buchanan, Appl. Phys. Lett. **40**, 675 (1982).

¹⁵J. M. Rowell, M. Gurvitch, and J. Geerk, Phys. Rev. B (in press).

¹⁶K. R. Milkove, J. Bostock, and M. L. A. MacVicar, Solid State Commun. **19**, 1095 (1976).

¹⁷D. H. Dye, D. P. Karim, J. B. Ketterson, and G. W. Crabtree, in *Transition Metals, 1977*, in Vol. 39 of *Institute of Physics Conference Series*, edited by M. J. G. Lee, J. M. Perz, and E. Fawcett (The Institute of Physics, Bristol, 1978), p. 683.

¹⁸G. Beuermann, Z. Phys. B **44**, 29 (1981).

¹⁹J. E. Dowman, M. L. A. MacVicar, and J. R. Waldram, Phys. Rev. **186**, 452 (1969).

²⁰J. P. Carbotte, in *Anisotropy Effects in Superconductors*, Ref. 5, p. 183.